

SiC AND MWCNT BLENDING ACTIONS ON FUNCTIONAL PERFORMANCE OF HYBRID AA2024 ALLOY NANOCOMPOSITE VIA TWO STEP STIR CAST ROUTE

M. Aruna

Department of Industrial Management, Faculty of Business, Liwa College, Abu Dhabi, UAE

S. Kaliappan

Division of Research and Development, Lovely Professional University, Jalandhar - Delhi, G.T. Road, Phagwara, Punjab 144411, India

D. V. V. S. B. Reddy Saragada

Department of Mechanical Engineering, Aditya Engineering College (A), Surampalem, Andhra Pradesh 533437, India

R. Venkatesh 

Department of Mechanical Engineering, Saveetha School of Engineering, Saveetha Institute of Medical and Technical Sciences (SIMATS), Saveetha University, Chennai, Tamilnadu 602105, India

V. Vijayan

Department of Mechanical Engineering, K.Ramakrishnan College of Technology, Trichy, Tamilnadu 621112, India

Manzoore Elahi M. Soudagar

Department of Mechanical Engineering, Graphic Era (Deemed to be University), Dehradun, Uttarakhand 248002, India

V. Mohanavel

Centre for Materials Engineering and Regenerative Medicine, Bharath Institute of Higher Education and Research, Chennai, Tamil Nadu 600073, India

Ismail Hossain

Department of Nuclear and Renewable Energy, Ural Federal University, Yekaterinburg, Russia 620002

A. H. Seikh

Mechanical Engineering Department, College of Engineering, King Saud University, 11421 Riyadh, Saudi Arabia

Copyright © 2024 American Foundry Society
<https://doi.org/10.1007/s40962-024-01351-3>

Abstract

The hybrid aluminium alloy matrix composites are adopted in high-strength-to-weight ratio applications with technical benefits, including high strength, good hardness, better stability, and improved thermal stability. This research is enhancing microstructural and mechanical functional behaviours of the hybrid aluminium alloy (AA2024) nanocomposites by the blending actions of nano silicon carbides (SiC) particles and multi-walled carbon nanotube (MWCNT) via a two-step stir cast route. The contribution effect of SiC and MWCNT blending actions on

metallography, physical/mechanical qualities, and resistance to corrosion individualities of hybrid AA2024 nanocomposites are studied by the procedure of the American Society for Testing and Materials (ASTM) and compared to monolithic cast AA2024 alloy characteristics. The hybrid AA2024 nanocomposite blended with SiC and MWCNT (weight percentages of 5 and 8%) exposed the specific tailored benefits like homogenous scattered reinforcements resulting in a lower percentage value of porosity ($\leq 1\%$), excellent ultimate tensile strength of 330 MPa with acceptable elongation range of 10%, enhanced indentation resistance capabilities of 128 HV, specific toughness of 15.2 J/mm², and enhanced corrosion performance.

Received: 17 January 2024 / Accepted: 07 April 2024
Published online: 07 May 2024

Keywords: AA2024, performance study, SiC, two-step stir cast, MWCNT

Introduction

Suchart Siengchin¹ and Kumar et al.² reported that the revolution of material series and the new class composites are the future trends for aerospace, automotive, sports equipment, defence, and structural industries for the specific key features of mechanical, thermal, and wear characteristics. The monolithic material embedded with metallic particles,³ fibre,⁴ and ceramic-based particulate⁵ through powder metallurgy,⁵ casting,⁶ and extrusion process⁷ resulting in enhanced mechanical, wear, corrosion, and thermal behaviour reported by Khalid et al.⁸ Singh et al.⁹ summarized that aluminium alloy composites are the current trend, and several research studies have been conducted to obtain the key benefits of monolithic cast alloy materials. Chandradass et al.¹⁰ recommended the liquid metallurgy processing is economical, efficient, and can make complex structures.

Shayan et al.¹¹ studied the exposure of titanium dioxide (TiO₂), the aluminium alloy (AA2024) nanocomposite was established by the process of stir casting and involved metallography and mechanical characteristic measurements which resulted in identifying the dendrite space between the particles, and excellent improvement in tensile, hardness, and elongation qualities related to monolithic AA2024 alloy. Farajollahi et al.¹² studied the quality of stir-cast processed AA2024 alloy composite intermetallic, mechanical, & abrasion performance and the metallographic structure interdendritic grain region containing more than 1.5 wt% of nickel. During the homogenization process treatment, the interdendritic region was limited and exposed to better mechanical/abrasion performance. Besides, the AA2024 alloy composite spots the agglomeration particle and microporosity by the consequences of air entrapment. Shin et al.¹³ studied the silicon carbide (SiC) dispersion and casting (die/stir) effect on porosity, cluster, tensile strength, and B scale hardness of AA2024 composites were measured by the 3, 6, and 9 volume percentage compositions. The die-cast synthesized composites had better metallographic qualities and mechanical performance than the stir-cast-made AA2024 composite. Kumar et al.¹⁴ composed hybrid AA7075 alloy composites with coconut shell ash and Al₂O₃ particles through two-step stir processing, offering the particle distribution as homogenous, resulting in superior tensile and abrasion resistance. At the same time, the higher loading content of Al₂O₃ was exhibited in reduced impact toughness. The corrosion behaviour and structural analysis of the hybrid AA2024 nanocomposite consisting of silicon (Si) and carbon nanotube (CNT) were evaluated by Muniyappan et al.¹⁵ through the electrochemical process using

varied solutions like HCl, H₂SO₄, and NaOH. The 4% Si and 4% CNT compositions exposed superior corrosion and better impedance. Besides, Kumar et al.¹⁶ summarized that utilizing CNT offered low density, and corrosion-analysed composites were involved in metallurgical analysis. With the assistance of stir casting—bottom pouring setup, the zirconium diboride incorporated aluminium alloy composite was developed, and the mechanical and corrosion performance was measured. It resulted in 15% and 26% improvement in tensile and impact strength (10 wt% of zirconium diboride) and good corrosion resistance. Akinwamide et al.¹⁷ prepared the aluminium hybrid composites by using silicon carbide (SiC) and ferrotitanium (TiFe) via a stir casting route, and its particle dispersion was identified as homogenous with enhanced microhardness. Using potentiodynamic polarization technology, the corrosion behaviour of composites was analysed and identified as 2% TiFe and 5% SiC, which have superior corrosion resistance values. Besides, Gnanavelbabu et al.¹⁸ and Kumar et al.¹⁹ reported that the AA2024 composite is enriched by adding alumina nanoparticles,^{18,19} and Shayan et al.²⁰ found high tensile/hardness on adding the silicon dioxide.²⁰ These composites can be recycled and utilized for new product manufacturing.²¹ Recently, Chandla et al.²² reviewed the stir-cast-made Al2024 alloy composite, and Al2024 is considered the prime matrix, and the optimum behaviour of the AA2024/5 wt% of SiC/2 wt% of Al₂O₃ alloy composite involves complex shape synthesis. Shin and Bae²³ synthesized the Al2024 alloy composite with 4 vol% of MWCNT via a stir cast process and studied the tensile and fatigue behaviour of the composite. It results showed better tensile and improved fatigue strength of 2.5×10^6 cycles. Baghel et al.²³ synthesized and evaluated the microstructure of the MWCNT-developed Al6082 nanocomposite. Evaluated results of Al6082 nanocomposite with 0.9 wt% of MWCNT showed better particle distribution.

Moreover, the high temperature melting of AA2024 alloy found hot cracks, microporosity, and voids due to gas bubble formation. It may affect the composite properties. The novel research involves studying the functional performance of hybrid AA2024 alloy nanocomposite by the contributions of nano SiC and MWCNT through a two-step stir casting technique. The blending actions on metallography, structure, mechanical, and corrosion qualities of hybrid aluminium nanocomposites are measured by the American Society for Testing and Materials. The innovation of this paper is to limit the casting defect. It enriches the composite behaviour during the hybrid AA2024 alloy fabrication via two-step stir cast processes and develops a composite with suitable composition to achieve maximum mechanical properties. The optimum compositions of

AA2024 alloy hybrid nanocomposite are recommended for high strength-to-weight ratio applications like automotive roof frame applications.

Materials and Methods

Research Materials

The ingot form of AA2024 alloy (30 mm diameter by 20 mm long) was chosen as the matrix due to its distinct benefits of heat treatability, better fatigue resistance, superior strength, and castability.^{11,12} By the nature of high hardness, chemical inertness, better thermal stability, superior abrasion resistance, and enhanced melting point reasons,¹³ the 50 nanometer SiC particle was picked as the reinforcement phase. Likewise, the powder form MWCNT was chosen for its high aspect ratio, flexibility, extraordinary strength, and high thermal conductivity.^{4,9} Moreover, with the references of Shin et al.¹³ and Chandla et al.,²² the nano SiC is fixed as 5 wt% and 8 wt% of MWCNT is chosen according to references of Padmavathi et al.⁴ and Shin and Bae.²³ The compositions of AA2024 alloy¹¹ and the basic behaviour of matrix and reinforcement phase materials are described in Tables 1 and 2.

The X-ray diffraction analysis looked at the grain size and crystal structure of nano SiC and MWCNT. The X-ray diffraction analysis pattern of SiC and MWCNT is highlighted in Figure 1.

Hybrid AA2024 Alloy Nanocomposite Fabrication

Hybrid AA2024 alloy nanocomposites were established using a two-step stir cast processing route, as displayed in Figure 2a. Here, the ingot form of AA2024 alloy of 589.5 g

is loaded into an electrical furnace and treated at 500°C. Likewise, the 50 nm SiC and 40 nm MWCNT are gathered as per wt% mentioned in Table 3 and held by a muffle furnace at 350°C for the preheating process, which helps to eliminate the moisture content.^{6,7}

The AA2024 ingot is placed in an electrical furnace temperature at 700°C under an argon atmosphere to assist in melting the alloy and limit the oxidation.¹⁰ Its setup is shown in Figure 2b. Once the liquid stage is obtained, the AA2024 bath is uniformly stirred, which helps to degas and prevent localized hot spots. Then, the temperature is reduced to 560°C, facilitating homogeneous particle dispersion and limiting air entrapment.¹⁴ The liquidus temperature for AA2024 alloy ranges from 600 to 640°C. So, if the liquidus temperature is 640°C, then melting it at 600°C would mean a superheat of 40°C. The total volume fraction of the solid is 90cc (casting).

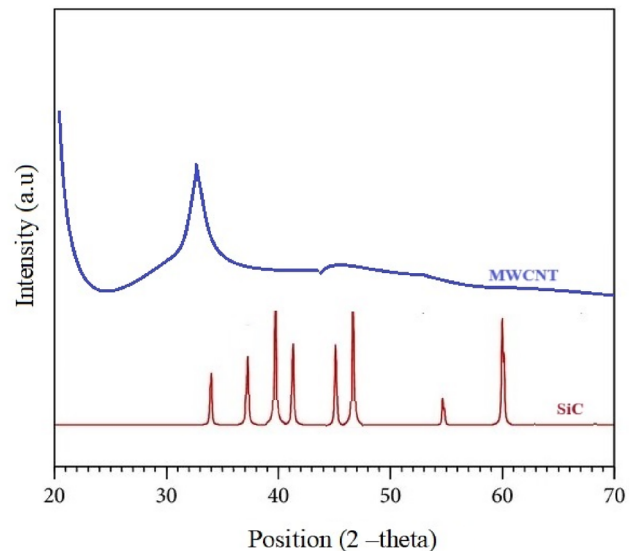


Figure 1. The X-ray diffraction patterns for SiC and MWCNT.

Table 1. Elemental Compositions of AA2024 Alloy

Elements properties	Al	Cu	Cr	Fe	Mn	Mg	Ti	Si	Zn
Weight percentage (wt%)	92.1	3.9	0.1	0.5	0.7	1.8	0.15	0.5	0.25

Table 2. Physical Characteristics of AA2024, SiC and MWCNT

Materials	Density g/cc	Melting point temperature °C	Modulus of elasticity GPa	Size
AA2024	2.78	502–638	73.1	30 mm × 20 mm
SiC	3.21	2797	410	50 nm
MWCNT	1.85	3652–3697	1800	40 nm

Meanwhile, the muffle furnace heated reinforcements are dropped into the molten metal through a feeder unit, as shown in Figure 2. The molten metal temperature is measured by a thermocouple and controlled by 560–590°C through the control panel. The semisolid state molten metal and the incorporated nano SiC& MWCNT are stirred by uniform stir speed 350 rpm for 5 min stir processing, as evidenced in Figure 2c. It supports very good particle distribution.¹⁴ Moreover, the higher content of MWCNT may change to agglomeration due to oxidation, which is controlled by an inert nature and applied uniform stir speed of 350 rpm. The well-mixed slurry dropped into a pre-heated (300°C) cylindrical die (3 cm diameter and 30 cm length of tool steel die). The synthesized composite specimens are illustrated in Figure 2d.

Characterization Qualities of Composites

The cast AA2024 alloy, AN1, AN2, and AHN composite specimens were involved in metallographic analysis,

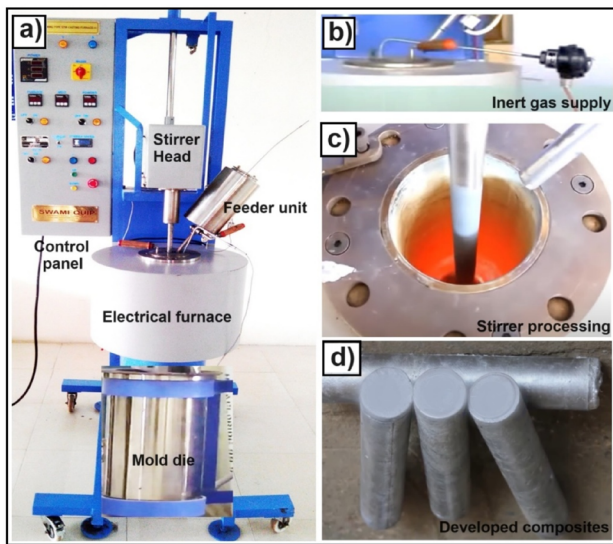


Figure 2. Fabrications setup (a) actual stir cast setup, (b) inert gas supply setup, (c) stirring of molten metal, and (d) synthesized composite samples.

Table 3. Compositions Details for Matrix and Reinforcements

Identification of composite	Composition details in wt%		
	AA2024	SiC	MWCNT
Cast AA2024	100	0	0
AN1	95	5	0
AN2	92	0	8
AHN	87	5	8

mechanical performance, and corrosion characterization were investigated, and the equipment, measuring, and ASTM standard details are addressed below. Figure 3 indicates the dimensioned cutting diagram showing where the specimens were extracted as it related to the filling direction.

Metallography Analysis

The VEGA3-TESCAN scanning electron microscope equipped with INCA software was utilized for metallography analysis. This SEM is capable of operating in both low and high vacuum modes, LaB6 filament utilized with best resolution of 2 nm at 30 kV. The composite specimens were prepared by a 1 cm cubic shape fine polished surface⁴ and etching by keller's reagent for examination purposes.

Density (Actual/Theoretical) and Porosity (%)

Based on the rule of mixture and Archimedes principle, the density (theoretical) and density (actual) are calculated by using Eqn 1 and 2.⁴ The weight composite is measured by a weighing machine (before being immersed in water fluid) noted by W_a and immersed in water fluid weighted by W_b . The porosity (%) of the composite is calculated by using Eqn 3.¹⁰

$$\text{Density(theoretical)} = daVa + dbVb \quad \text{Eqn. 1}$$

where da/db is the density of matrix/reinforcement, and Va/Vb is the volume of matrix/reinforcements.

$$\text{Density(actual)} = \frac{Wa}{Wa - Wb} \times \text{density of water} \quad \text{Eqn. 2}$$

$$\text{Porosity percentage} = 1 - \frac{\text{Density(actual)}}{\text{Density(theoretical)}} \times 100 \quad \text{Eqn. 3}$$

Mechanical Performance

According to ASTM E23 (5.5 cm × 1 cm × 1 cm), E8 (10 cm × 1 cm × 0.6 cm), and E384-99 (6 cm × 22 cm) standards, the composite's impact toughness, tensile strength performance, and microhardness are measured. A Fuel Instruments & Engineers Pvt. Ltd. Charpy impact tester, universal testing machine (5 mm/min feed rate), and VM30 model Vickers hardness tester (load-100 g & duration-15 s) are utilized for performing the above-mentioned mechanical tests. Besides, the three test trials are executed from each composite specimen, and the three trials' mean is considered the final value with a maximum error margin of 5%.

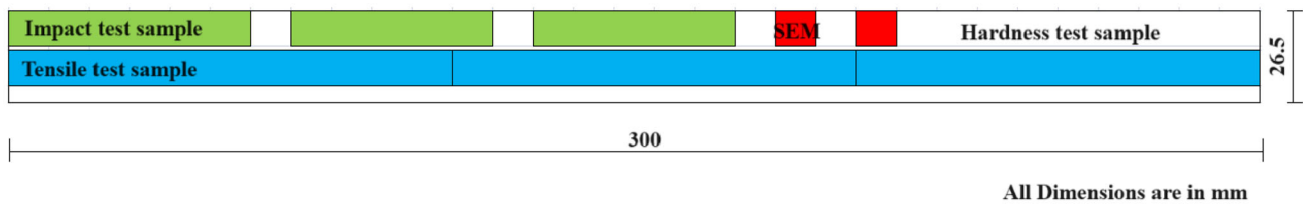


Figure 3. Dimensioned cutting diagram for test samples.

Corrosion Performance

The developed composite specimens were analysed using the electrochemical corrosion test. With the adaptation of open circuit potential, the composite specimen treated as anode terminal and platinum base considered as cathode terminal (current density- 2 mA/cm², oscillation -20 mV, NaCl-3.5%, and intensity spectrum - 1 × 10⁻⁵ HZ). Moreover, the corrosion rate is calculated by the weight loss method and mentioned in Eqn 4.¹⁵

$$\text{Corrosion Rate} = 87.6 \frac{W}{DAT} \quad \text{Eqn. 4}$$

where W is weight loss in milligrams, D is the metal density in g/cc, A is the area of the composite test sample in cm², and T is the exposures of the metal sample in hours.

Results and Discussion

The output results of the synthesized composite specimen's surface morphology, density/porosity, impact toughness, tensile performance, microhardness, and corrosion performance are detailed as follows.

Metallography Analysis

The scanning electron microscope-Energy-dispersive X-ray spectroscopy (SEM-EDS) of AA2024 cast alloy, AA2024/5 wt% SiC, AA2024/8 wt% MWCNT, and AA2024/5 wt% SiC/8 wt% MWCNT is shown in Figure 4a-d.

Here, Figure 4a is evidence of the surface morphology of cast AA2024 alloy with few voids noted in the surface and dendrite structure. The semisolid state stir processing is why dendrite grains have an intermetallic phase of Al₃Si. The nano SiC particles incorporated AA2024 alloy nanocomposite made by two-step stir processing and have better particle dispersion with limited microvoids, presented in Figure 4b. It shows that SiC particle distribution is homogenous and maintains the coarse grain structure, resulting in better resistance to indentation.^{12,14} The major black visible mark identified from Figure 4b is a nano SiC particle that conforms its appearance in the AA2024 matrix as good interfacial bonding.

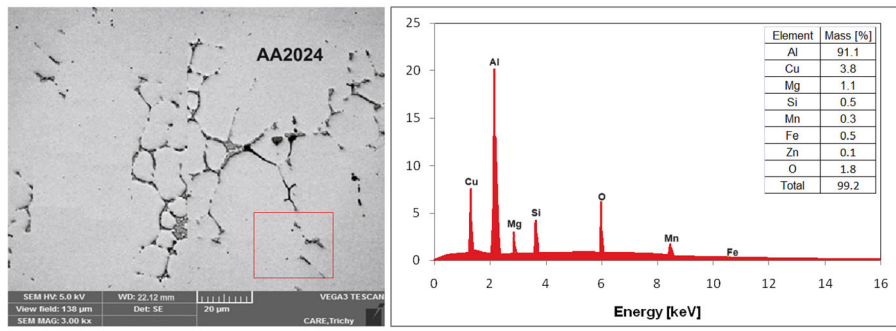
Likewise, the MWCNT included AA2024 alloy composite (AN2), which is exposed in Figure 4c. The MWCNT is distributed uniformly with improved particle distance, which may affect the interface behaviour and chances of reducing the mechanical performance.⁴ Moreover, the MWCNT makes an efficient interface bonding, as highlighted in Figure 4c.

In addition, this structure had a few identical microvoids and porosity, and its range of porosity is experimentally proved in Figure 4. With the support of Figure 4d, the metallography image of hybrid AA2024 alloy nanocomposite composed of nano SiC and MWCNT is exposed to homogenous particle dispersion in AA2024 alloy matrix at equally distanced particles. The two-step stir processing at constant stir speed is the reason for homogenous particle dispersion,¹² which results in superior mechanical and abrasion characteristics.¹⁴ The semisolid state processed hybrid AA2024 alloy composite conforms to the SiC and MWCNT, which shows better interfacial bonding with the base matrix, as evidenced in Figure 4d.

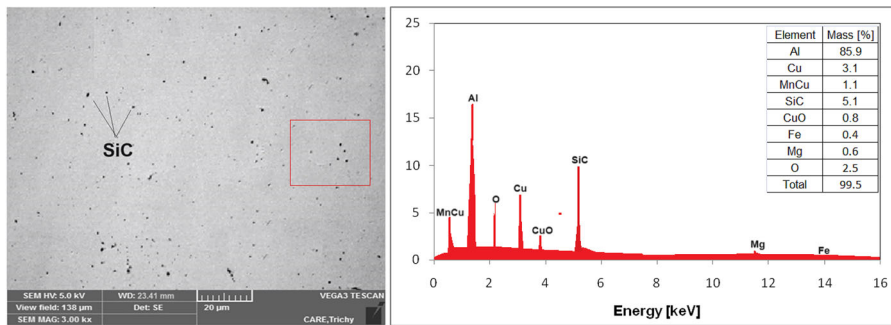
Density/Porosity Performance of Composites

Figure 5 bar chart indicates the density/porosity of synthesized cast AA2024 alloy, AN1, AN2, and AHN. It illustrates the variations in density with the declined level of composite porosity. Besides, composite specimens' density (theoretical) is greater than the density (actual) value. The unavoidable internal microporous is the reason for the reduced density (actual) of the composite⁵ and the level of porosity spotted as ≤1%.

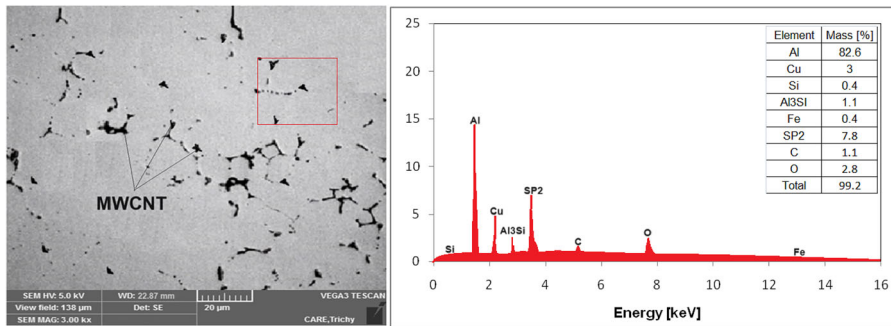
The density (actual) of cast AA2024 alloy is 2.75±0.05 g/cc, and the inclusions of nano SiC in the AA2024 alloy matrix are exposed by 2.77±0.07 g/cc. However, the incorporations of MWCNT in AA2024 are obtainable as 2.68 g/cc because the individual density of MWCNT is 1.85 g/cc, which was lower than the matrix material, and its density value comparison is mentioned in Table 2. Likewise, the AHN composite's density (actual) of 2.70±0.06 g/cc follows the rule of mixture.² The same approach was expressed by Padmavathi et al.⁴ while measuring Hybrid AZ91D alloy nanocomposite consisting of nano SiC and CNT. However, the AHN composite (AA2024/5 wt% SiC/



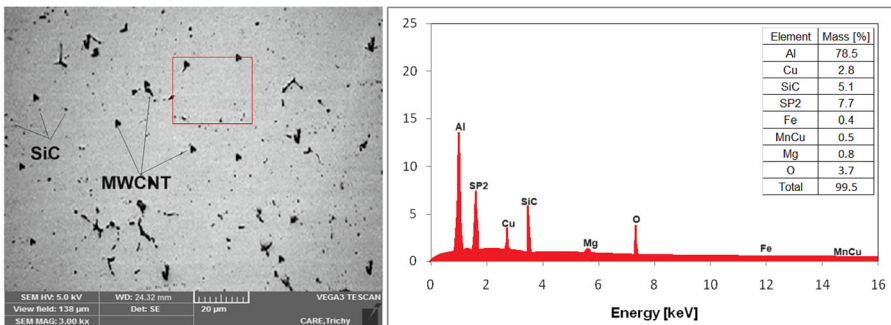
(a)



(b)



(c)



(d)

Figure 4. (a) The SEM-EDS image of cast AA2024. (b) SEM-EDS image of AN1 (AA2024/5 wt% SiC). (c) SEM-EDS image of AN2 (AA2024/8 wt% MWCNT). (d) SEM-EDS image of AHN (AA2024/5 wt% SiC/8 wt% MWCNT).

8 wt% MWCNT) spots the optimum density/porosity, and its values are lesser than the density/porosity values of cast AA2024 alloy.

The calculated porosity of cast AA2024 alloy is 0.97%, lower than the conventional liquid stir-developed aluminium alloy cast.⁵ The argon inert gas reduces oxidation during the high-temperature melt,¹⁰ causing reduced porosity (%). Moreover, the additions of 5 wt% nano SiC, 8 wt% of MWCNT, and 5 wt% SiC/8 wt% MWCNT exhibited reduced porosity (%) of 0.91, 0.87, and 0.85%, respectively. The two-step stir casting process, including high-temperature melts and reinforcements, blended with molten metal in a semisolid state under an inert atmosphere, limits the gas bubble and oxide formation and causes reduced casting defects, including hot cracks, voids, and porosity.

Mechanical Qualities of Composites

According to ASTM E8 policy, the tensile tested cast AA2024 alloy, AN1, AN2, and AHN composite are exposed with their elongation (%) in Figure 6. Composite yield and tensile strength, elongation percentage and modulus of elasticity are mentioned in Table 4.

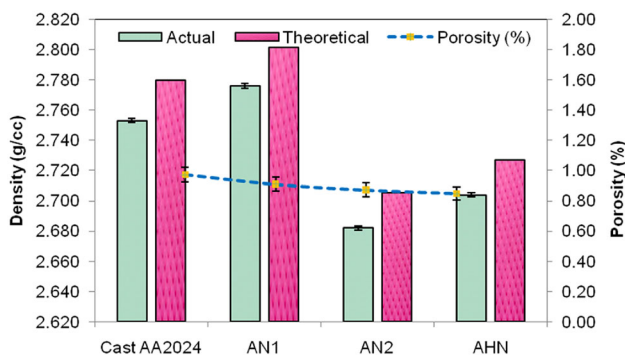


Figure 5. Density/porosity of synthesized composites.

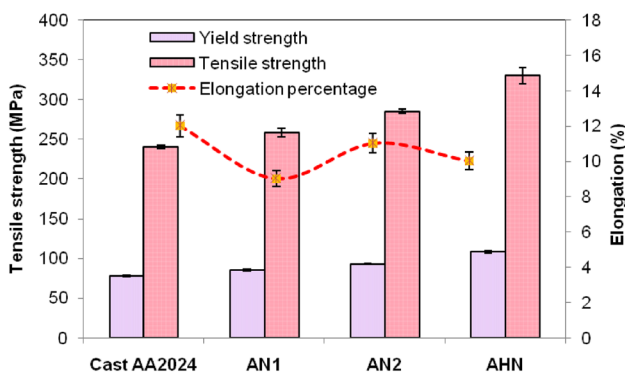


Figure 6. Yield/tensile/elongation (%) of synthesized composites.

The tensile performance of composite specimens exhibited high tensile strength on the mono and multi-reinforcements loading. The tensile value of 240 ± 2.5 MPa is observed by the specimen of cast AA2024 alloy made without reinforcement, and its value reaches the standard tensile stress value.^{12,15}

The loading of mono reinforcements like nano SiC and MWCNT in the AA2024 alloy matrix (AN1 and AN2) is measured to be 258 ± 5.2 MPa and 285 ± 2.9 MPa, respectively. The sufficient bonding capabilities between the AA2024 and nano SiC particle cause better tensile strength, which is improved by 7.5% related to cast AA2024 alloy. Besides, by the appearance, MWCNT in AA2024 alloy matrix exhibited the maximum tensile strength and hiked by 18.75% for the reasons of uniform particle dispersion with adhesive actions made with dendrite AA2024 alloy grain as highlighted in Figure 4c. The effective blending action and stir process parameter may fix the qualities of the composite.¹² However, the AHN hybrid AA2024 alloy nanocomposite liberates the peak tensile strength of 330 ± 6.5 MPa and attained 37.5% improvement related to cast AA2024 alloy. This composite is compared with past literature. It is exposed by 5.1% greater tensile strength.¹³ In addition, the elongation percentages of composites show variations due to the loading effect of nano SiC and MWCNT. The AHN composite has its own 10% elongation rate, which is lower than the value of cast AA2024

Table 4. Tensile Characteristics of Composites

Identification of composite	Yield strength MPa	Tensile strength MPa	Elongation %	Modulus of elasticity GPa
Cast AA2024	78 ± 1.1	240 ± 2.5	12 ± 0.2	72 ± 2
AN1	85 ± 1.5	258 ± 5.2	9 ± 0.1	67 ± 1
AN2	93 ± 1	285 ± 2.9	11 ± 0.2	71 ± 1.5
AHN	108 ± 1.3	330 ± 6.5	10 ± 0.2	70 ± 2

alloy. Based on the ceramic particle loading, the elongation

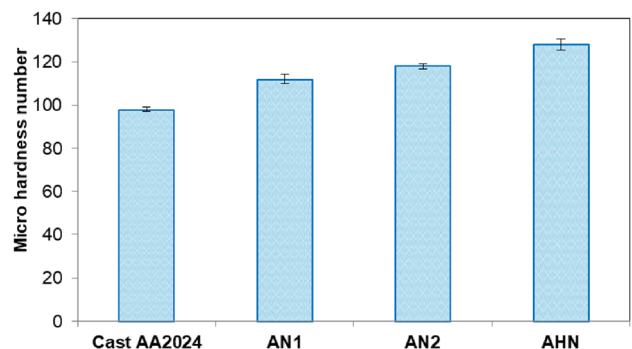


Figure 7. Vickers hardness of synthesized composites.

percentage was reduced with enhanced tensile strength due to efficient bonding strength.^{4,10,12}

With the exposure of Figure 7, the microhardness of AA2024 alloy composite made with/without reinforcement phase is identified as better results, and the microhardness of cast AA2024 alloy is 98 ± 1 HV and the exposure of 5 wt% nano SiC particle in AA2024 alloy is measured by 112 ± 2.24 HV. The coarse grain with distributed homogenous particles could resist the indentation and endure the peak load and its surface, as shown in Figure 4(b). This hardness value is 7% greater than the previously reported value.¹¹

The loading of 8 wt% MWCNT in the AA2024 alloy matrix is 118 ± 1.1 HV, greater than the cast A2024 alloy and AN1 nanocomposite. Generally, the CNT has better mechanical and thermal performance.¹⁵ The highest microhardness value of 128 ± 2.5 HV is observed by the AHN composite made by using 5 wt% nano SiC and 8 wt% MWCNT. The effective reinforcement combination in AA2024 alloy with superior interfacial bonding strength is the reason for maximum hardness. Compared to the AA2024 alloy cast, it was enhanced by 30.6%.

Cast AA2024 alloy, AN1, AN2, and AHN composite impact toughness performance is displayed in Figure 8 with a 5% allowable error. The inclusion of hybrid reinforcements notes a significant hike. The impact toughness of AA2024 alloy cast liberates 11.1 ± 0.24 J/mm² and improves to 12.2 J/mm² by incorporating 5 wt% nano SiC particle. As mentioned earlier, the AZ91D alloy composite exposed a better toughness value and an improved loading content of nano SiC.⁴

The impact toughness of the AN2 composite is 13.51 ± 0.3 J/mm² and greater than the impact toughness value of the AA2024 alloy and AN1 composite specimen. The AHN composite is spotted by the highest impact toughness value of 15.27 ± 0.5 J/mm². Compared to cast AA2024 and AN2 composite, it has hiked by 35.64% and 13%, respectively.

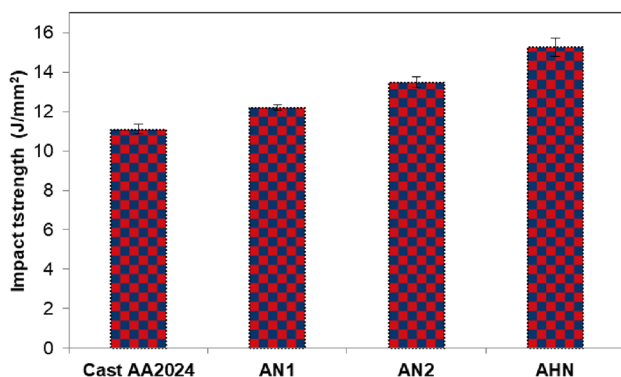


Figure 8. Impact toughness of synthesized composites.

Table 5. Polarization Investigation Results

Synthesized AA2024 composites	Potential (V)	E_{corr} (V)	Current (I_{corr} -mA/cm ²)	Corrosion (mm/year)
Cast AA2024 alloy	-0.9561	-0.9218	0.9619	9.13
AN1	-1.1213	-1.0516	0.5719	7.12
AN2	-1.1312	-1.0519	0.5698	6.74
AHN	-0.9915	-0.9913	0.1417	3.23

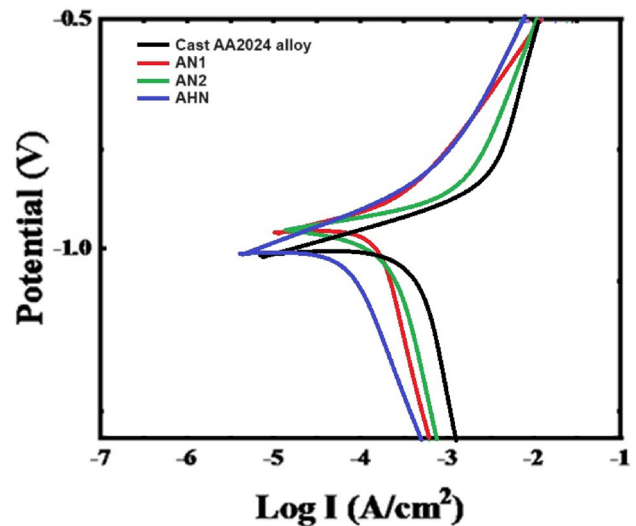


Figure 9. Polarization plot for synthesized composites.

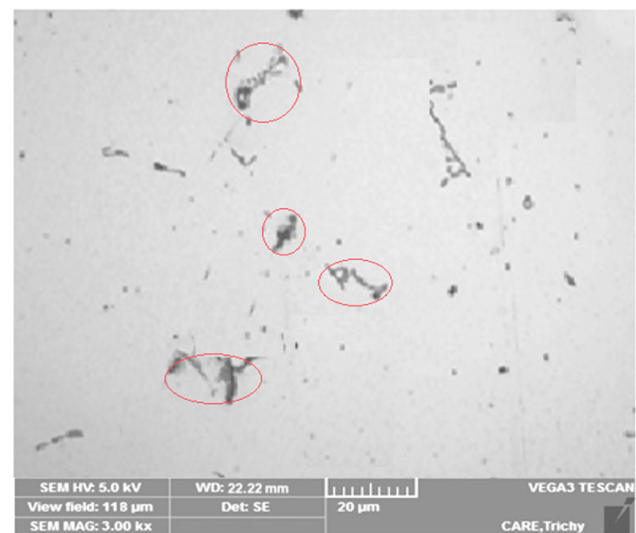


Figure 10. Corrosion morphology of AHN (AA2024/5 wt% SiC/8 wt% MWCNT).

Table 6. Summary Comparison of Present Results to Past Literature

S.No	Details of composite	Yield strength MPa	Tensile strength MPa	Vickers hardness HV	Impact toughness J/mm ²	Corrosion mm/year	References
1	AZ91D/6 wt% SiC/6 wt% CNT	150	241	78	–	–	4
2	AA2024/1 vol% TiO ₂	142	235	95BHN	–	–	12
3	AA2024/4% CNT/2% Silicon	–	–	–	–	1.1	15
4	AA2024/5 wt% SiC/8 wt% MWCNT	108	330	128	15.27	3.23	Present work

The homogenous particle dispersion and coarse grain microstructure are the reason for high impact toughness.

Corrosion Resistance Performance

The corrosion performance analysis results are detailed in Table 5 and consist of potential, current, and corrosion rates (mm/year).

Here, Figure 9 illustrates the corrosion behaviour of cast AA2024, AN1, AN2, and AHN composites measured by 3.5% NaCl solutions. The corrosion rate of cast AA2024 alloy is 9.13 mm/year, and the incorporation of 5 wt% nano SiC in the AA2024 alloy matrix owns a 7.12 mm/year corrosion rate, less than the cast AA2024 alloy. The appearance of SiC may resist the corrosion effect against the NaCl solutions. An earlier study reported the same approach.¹⁶ Moreover, including 8 wt% MWCNT in AA2024 alloy enhanced the corrosion resistance, and its value is 6.74 mm/year under the potential of -1.1312 V. The lowest corrosion rate of 3.23 mm/year is monitored by the composite made with 5 wt% nano SiC and 8 wt% MWCNT through a two-step stir-cast process.

Figure 10 exposes the corrosion morphology of hybrid AA2024 alloy composite embedded with 5 wt% nano SiC and 8 wt% MWCNT. The red corrosion-affected area and the small pit galvanic corrosion surface were sacrificed due to active metal under an electrochemical corrosion test.¹⁵ Besides, the combinations of SiC and MWCNT with better interfacial bonding are the reason for lower corrosion resistance compared to others.

Table 6 indicates the summary comparison of present investigation results with past reported values. The present developed hybrid AA2024 alloy composite embedded with 5 wt% SiC and 8 wt% MWCNT has higher tensile strength (330 MPa) and 40% improved tensile strength value of AA2024/1 vol% TiO₂ developed composite.¹² The hardness of AA2024/5 wt% SiC/8 wt% MWCNT hybrid composite is enriched by 64% related to AZ91D/6 wt%

SiC/ 6 wt% CNT hybrid composites. Similarly, the hybrid AA2024/5 wt% SiC/8 wt% MWCNT composite showed better impact strength of 15.27 J/mm², 37.56% higher than the monolithic AA2024 cast alloy. But, the corrosion behaviour of composite is showed 3.23 mm/year. It is higher than the corrosion rate of the past reported value of 1.1 mm/year.¹⁵ With this concern, further research will change the reinforcement composition and study its mechanical/corrosion behaviour.

Conclusions

The two-step stir cast process adopted for the synthesis of the AA2024 alloy composite consists of 5 wt% SiC, 8 wt% MWCNT, and 5 wt% SiC/8 wt% MWCNT was effectively fabricated and its metallography, physical/mechanical qualities, and resistance to corrosion individualities of hybrid AA2024 nanocomposites were experimentally investigated by the ASTM policy. The key findings are summarized as follows:

- The surface morphology of two-step stir cast processing for AA2024 alloy and its composite shows few voids and a homogenous particle distribution.
- Amid the different compositions of AA2024 alloy composites, the AHN (AA2024/5 wt% SiC/8 wt% MWCNT) hybrid nanocomposite performed better regarding physical/mechanical and corrosion behaviour.
- The AHN spot has the lowest porosity of 0.85% with an optimum density (actual) of 2.70 g/cc.
- The AHN has specific tensile, microhardness, and impact toughness, which is improved by 37.5%, 30.61% and 37.56% related to monolithic cast AA2024 alloy.
- Likewise, the AHN composite specimen facilitated a low corrosion rate and was limited by 182% rather than cast AA2024 alloy.
- In the future, the optimum composite will be involved in machinability studies. The developed composite can be recycled.

Acknowledgements

The authors would like to acknowledge the Researchers Supporting Project number (RSP2024R373), King Saud University, Riyadh, Saudi Arabia.

Author Contributions

All the authors contributed to the study's conception and design. Material preparation, data collection and analysis were carried out by M. Aruna, S. Kaliappan, A. Mohana Krishnan, Venkatesh R, V. Vijayan, Manzoore Elahi M. Soudagar, V. Mohanavel, Sulaiman Ali Alharbi and A. H. Seikh. The first manuscript draft was prepared by [R. Venkatesh] and subsequently, all the authors contributed to the finalization of the manuscript.

Funding

The authors did not receive support, including funds, from any organization for the submitted work. No funding was received to assist with the preparation of this manuscript.

Data Availability

All the data required are available within the manuscript.

Competing interests The authors have no relevant financial or non-financial interests to disclose. The authors have no competing interests to declare relevant to this article's content. All authors certify that they have no affiliations with or involvement in any organization or entity with any financial or non-financial interest in the subject matter or materials discussed in this manuscript. The authors have no financial or proprietary interests in any material discussed in this article.

Ethics approval This is an observational study. SiC and MWCNT blending actions on functional performance of hybrid AA2024 alloy nanocomposite via two step stir cast route, Research Ethics Committee has confirmed that no ethical approval is required.

REFERENCES

1. S. Siengchin, A review on lightweight materials for defence applications: present and future developments. *Defence Technol.* **24**, 1–17 (2023). <https://doi.org/10.1016/j.dt.2023.02.025>
2. P. Kumar, S.K. Sharma, R.K.R. Singh, Recent trends and future outlooks in manufacturing methods and applications of FGM: a comprehensive review. *Mater. Manuf. Process.* **38**(9), 1033–1067 (2023). <https://doi.org/10.1080/10426914.2022.2075892>
3. L.J. Xu, F.N. Xiao, Y.C. Zhao, Y.C. Zhou, S.Z. Wei, Properties and microstructure of oxide dispersion strengthened tungsten alloy prepared by liquid-phase method: a review. *Tungsten* **5**, 481–502 (2023). <https://doi.org/10.1007/s42864-022-00180-3>
4. K.R. Padmavathi, R. Venkatesh, G.R. Devi, V. Muthukumar, Synthesis and characteristics evaluation of SiC_{np} and SiC_{np}/CNT-reinforced AZ91D alloy hybrid nanocomposites via semisolid stir casting technique. *Int. J. Metalcast.* (2023). <https://doi.org/10.1007/s40962-023-01137-z>
5. Y. Karabulut, R. Unal, Additive manufacturing of ceramic particle-reinforced aluminium-based metal matrix composites: a review. *J. Mater. Sci.* **57**, 19212–19242 (2022). <https://doi.org/10.1007/s10853-022-07850-0>
6. K.K. Sadhu, N. Mandal, R.R. Sahoo, SiC/graphene reinforced aluminium metal matrix composites prepared by powder metallurgy: a review. *J. Manuf. Process.* **91**, 10–43 (2023). <https://doi.org/10.1016/j.jmapro.2023.02.026>
7. S. Senthilkumar, K. Revathi, E. Sivaprakash, Enhancement of magnesium alloy (AZ31B) nanocomposite by the additions of zirconia nanoparticle via stir casting Technique: physical, microstructural, and mechanical behaviour. *Int. J. Metalcast.* (2023). <https://doi.org/10.1007/s40962-023-01116-4>
8. S.K. Sharma, K.K. Saxena, K.H. Salem, K.A. Mohammed, R. Singh, C. Prakash, Effects of various fabrication techniques on the mechanical characteristics of metal matrix composites: a review. *Adv. Mater. Process. Technol.* (2022). <https://doi.org/10.1080/2374068X.2022.2144276>
9. M.Y. Khalid, R. Umer, K.A. Khan, Review of recent trends and developments in aluminium 7075 alloy and its metal matrix composites (MMCs) for aircraft applications. *Results Eng.* **20**, 101372 (2023). <https://doi.org/10.1016/j.rineng.2023.101372>
10. B. Singh, I. Kumar, K.K. Saxena, K.A. Mohammed, M.I. Khan, S.B. Moussa, S.S. Abdullaev, A future prospects and current scenario of aluminium metal matrix composites characteristics. *Alex. Eng. J.* **76**, 1–17 (2023). <https://doi.org/10.1016/j.aej.2023.06.028>
11. J. Chandradass, T. Thirugnanasambandham, P.B. Sethupathi, Liquid state stir processing and characteristics study of AZ91D/SiCp composites. *Mater. Today Proc.* **45**, 6507–6511 (2021). <https://doi.org/10.1016/j.matpr.2020.11.450>
12. M. Shayan, B. Eghbali, B. Niroumand, Fabrication of AA2024–TiO₂ nanocomposites through stir casting process. *Trans. Nonferrous Metals Soc. China* **30**(11), 2891–2903 (2020). [https://doi.org/10.1016/S1003-6326\(20\)65429-2](https://doi.org/10.1016/S1003-6326(20)65429-2)
13. R. Farajollahi, H.J. Aval, R. Jamaati, Effects of Ni on the microstructure, mechanical and tribological properties of AA2024–Al₃NiCu composite fabricated by stir casting process. *J. Alloys Compd.* **887**, 161433 (2021). <https://doi.org/10.1016/j.jallcom.2021.161433>
14. S. Shin, H. Park, B. Park, S.B. Lee, S.K. Lee, Y. Kim, S. Cho, I. Jo, Dispersion mechanism and mechanical

- properties of SiC reinforcement in aluminium matrix composite through stir and die-casting processes. *Appl. Sci.* **11**, 952 (2021). <https://doi.org/10.3390/app11030952>
15. A. Kumar, R.C. Singh, R. Chaudhary, Investigation of nano- Al_2O_3 and micro-coconut shell ash (CSA) reinforced AA7075 hybrid metal–matrix composite using two-stage stir casting. *Arab. J. Sci. Eng.* **47**, 15559–15573 (2022). <https://doi.org/10.1007/s13369-022-06728-2>
 16. M. Muniyappan, N. Iyandurai, P. Duraisamy, Structural characterization and corrosion behaviour of AA 2024 reinforced with carbon nanotubes and silicon hybrid metal matrix nanocomposites. *Mater. Today Proc.* **43**, 1132–1140 (2021). <https://doi.org/10.1016/j.matpr.2020.08.600>
 17. S.D. Kumar, M. Ravichandran, A. Jeevika, B. Stalin, C. Kailasanathan, A. Karthick, Effect of ZrB_2 on microstructural, mechanical and corrosion behaviour of aluminium (AA1718) alloy matrix composite prepared by the stir casting route. *Ceram. Int.* **47**(9), 12951–12962 (2021). <https://doi.org/10.1016/j.ceramint.2021.01.158>
 18. S.O. Akinwamide, O.J. Akinribide, P.A. Olubambi, Influence of ferrotitanium and silicon carbide addition on structural modification, nano hardness and corrosion behaviour of stir-cast aluminium matrix composites. *SILICON* (2020). <https://doi.org/10.1007/s12633-020-00733-6>
 19. A. Gnanavelbabu, K.T.S. Surendran, S. Kumar, Process optimization and studies on mechanical characteristics of AA2014/ Al_2O_3 nanocomposites fabricated through ultrasonication assisted stir-squeeze casting. *Int. J. Metal Cast.* (2021). <https://doi.org/10.1007/s40962-021-00634-3>
 20. M. Kumar, R. Kumar, S. Bhaskar, Parametric optimization and ranking Analysis of Aa2024– Al_2O_3 / AlN alloy composites fabricated via stir casting route under dry sliding wear investigation. *Int. J. Metalcast.* (2023). <https://doi.org/10.1007/s40962-023-01053-2>
 21. M. Shayan, B. Eghbali, B. Niroumand, Synthesis and characterization of Aa2024– SiO_2 nanocomposites through the vortex method. *Int. J. Metalcast.* (2021). <https://doi.org/10.1007/s40962-021-00574-y>
 22. R.P. Barot, R.P. Desai, M.P. Sutaria, Recycling of aluminium matrix Composites (AMCs): a review and the way forward. *Int. J. Metal Cast.* **17**, 1899–1916 (2023). <https://doi.org/10.1007/s40962-022-00905-7>
 23. N.K. Chandla, S. Kant, M.M. Goud, A review on mechanical properties of stir cast Al-2024 metal matrix composites. *Adv. Mater. Process. Technol.* **9**(3), 948–969 (2023). <https://doi.org/10.1080/2374068X.2022.2106670>
 24. S.E. Shin, D.H. Bae, Fatigue behavior of Al2024 alloy-matrix nanocomposites reinforced with multi-walled carbon nanotubes. *Compos. B Eng.* **134**, 61–68 (2018). <https://doi.org/10.1016/j.compositesb.2017.09.034>
 25. M. Baghel, C.M. Krishna, Synthesis and characterization of MWCNTs/ Al6082 nanocomposites through ultrasonic assisted stir casting technique. *Part. Sci. Technol.* **41**(2), 183–195 (2023). <https://doi.org/10.1080/02726351.2022.2065651>

Publisher's Note Springer Nature remains neutral with regard to jurisdictional claims in published maps and institutional affiliations.

Springer Nature or its licensor (e.g. a society or other partner) holds exclusive rights to this article under a publishing agreement with the author(s) or other rightsholder(s); author self-archiving of the accepted manuscript version of this article is solely governed by the terms of such publishing agreement and applicable law.